

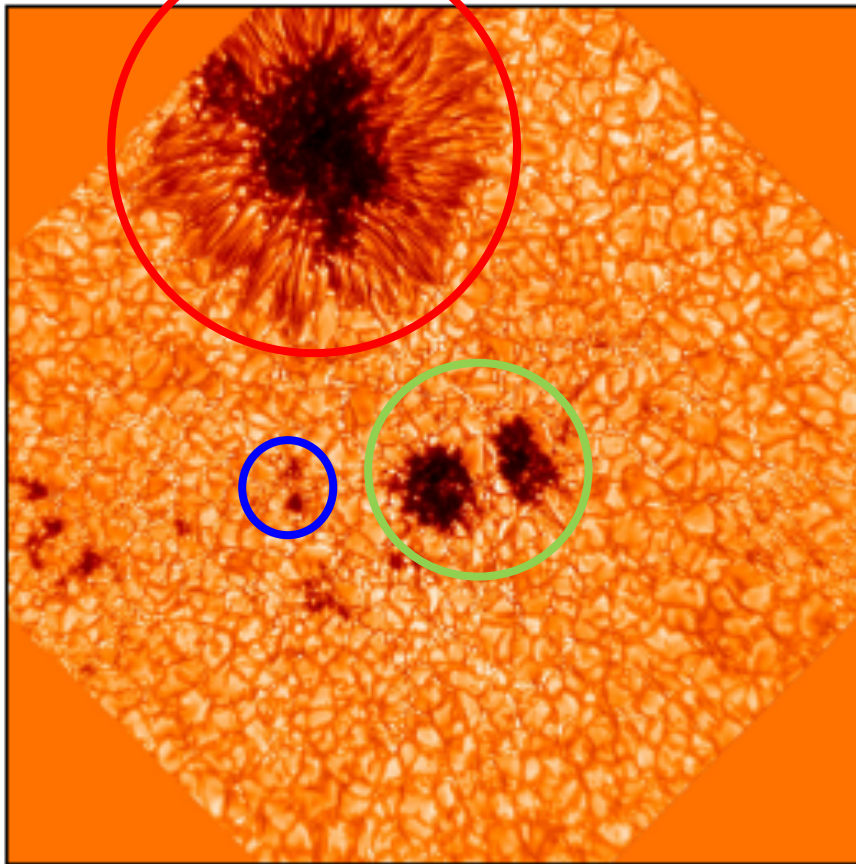
Observations of Umbra waves with NST and SDO

Kyung-Suk Cho (趙京錫)

Collaboration with S.-C. Bong , I.-H. Cho (KASI),
J.C. Chae (SNU), V. Nakariakov (KHU)

Sunspots

NST TiO band 2014-06-03T18:50:25



Mature Sunspots
(Penumbral Sunspots)

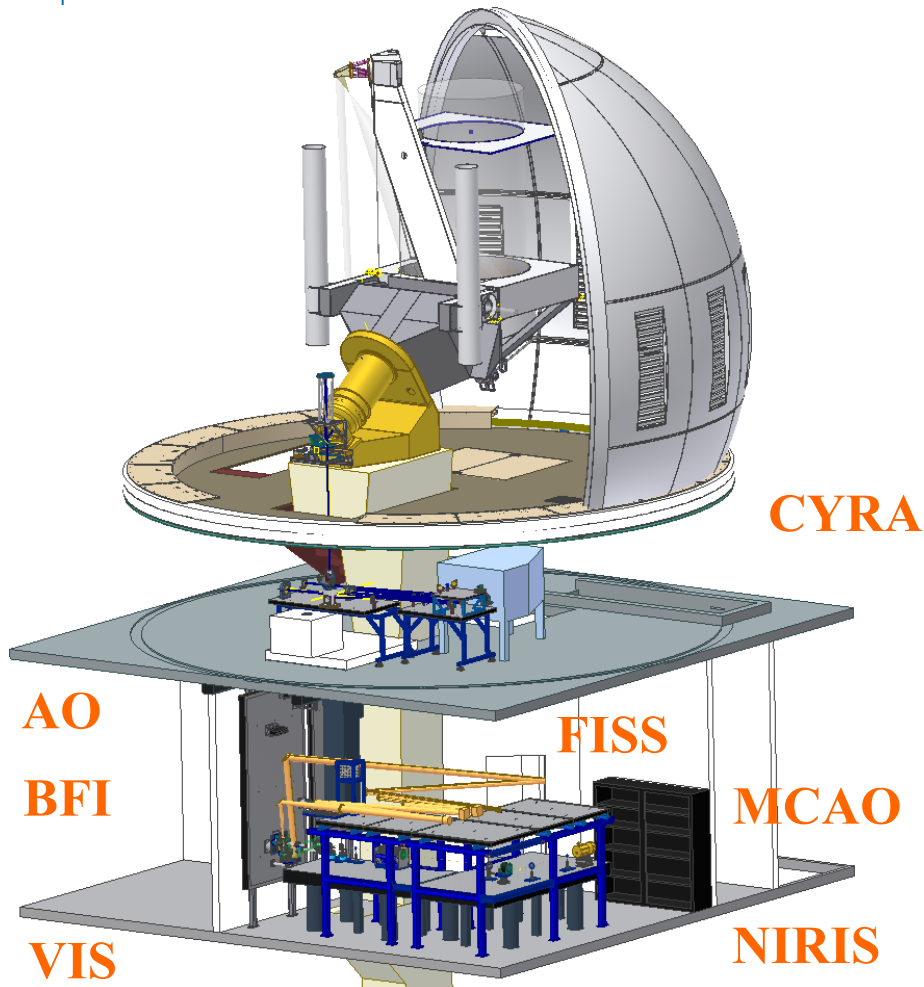
Transitional Sunspots

Pores
(Penumbra-less sunspots)

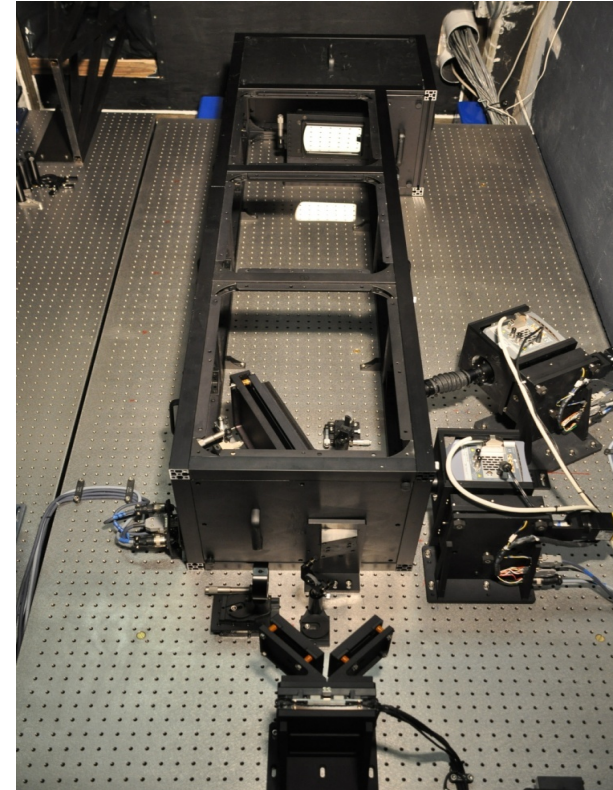
Tlatov & Pevstov (2014)



(1) Intensity and Doppler
Oscillations in Pore Atmosphere
using NST



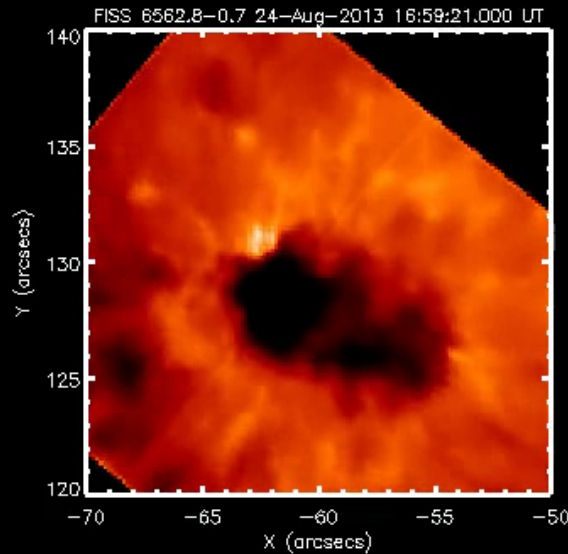
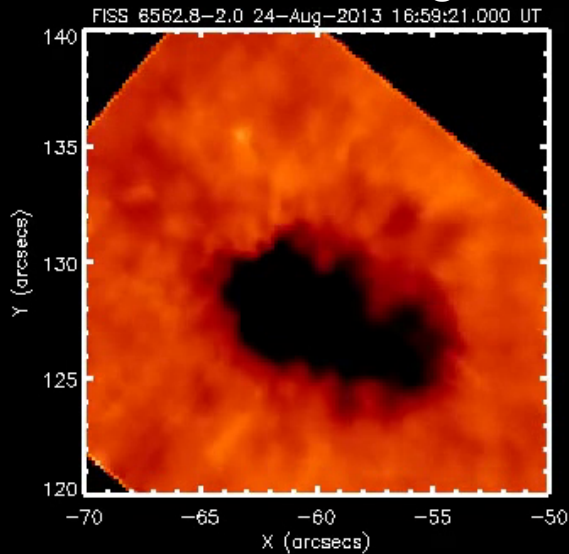
Fast Imaging Solar Spectrograph (FISS)



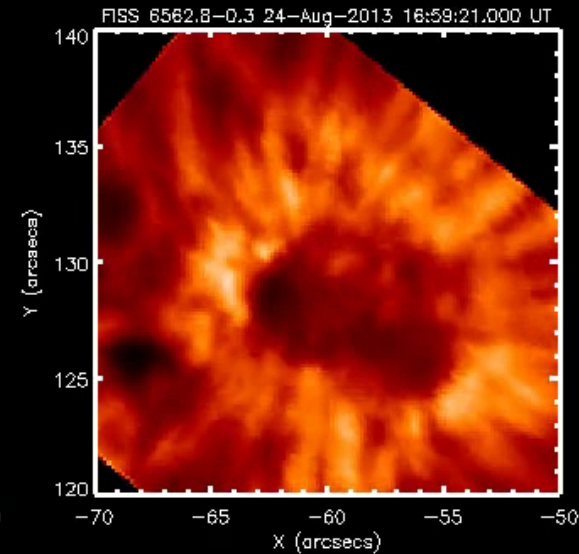
FISS is a unique system that can do imaging of H-alpha and Ca II 8542 band simultaneously, which is quite suitable for studying of dynamics of chromosphere.

FISS Ha Intensity

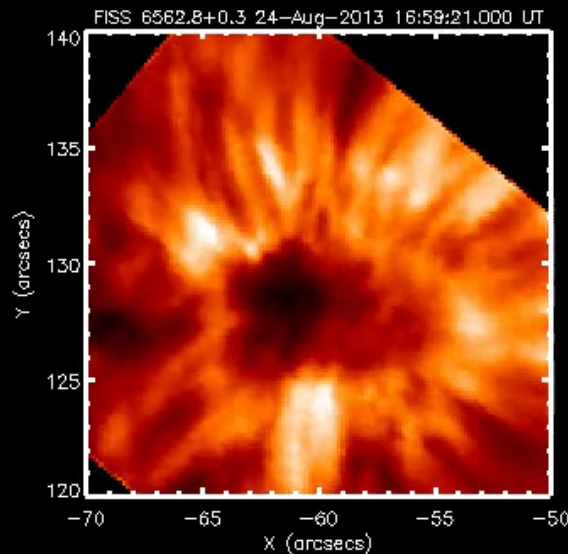
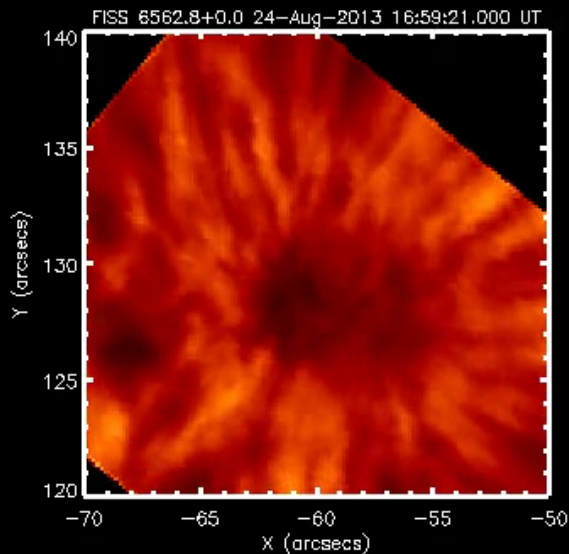
Ha Line wing



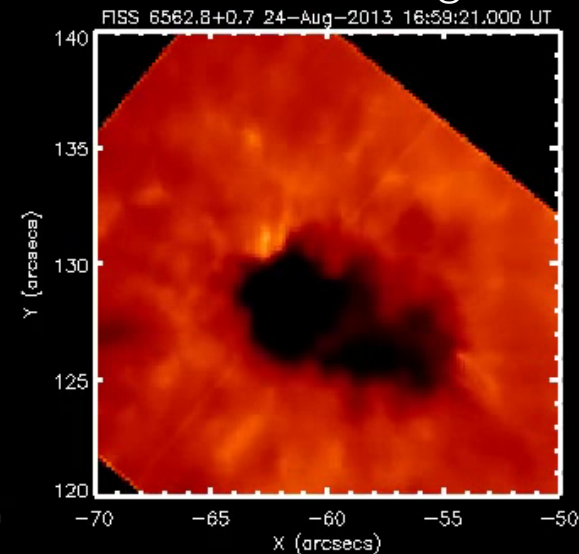
Ha Line core



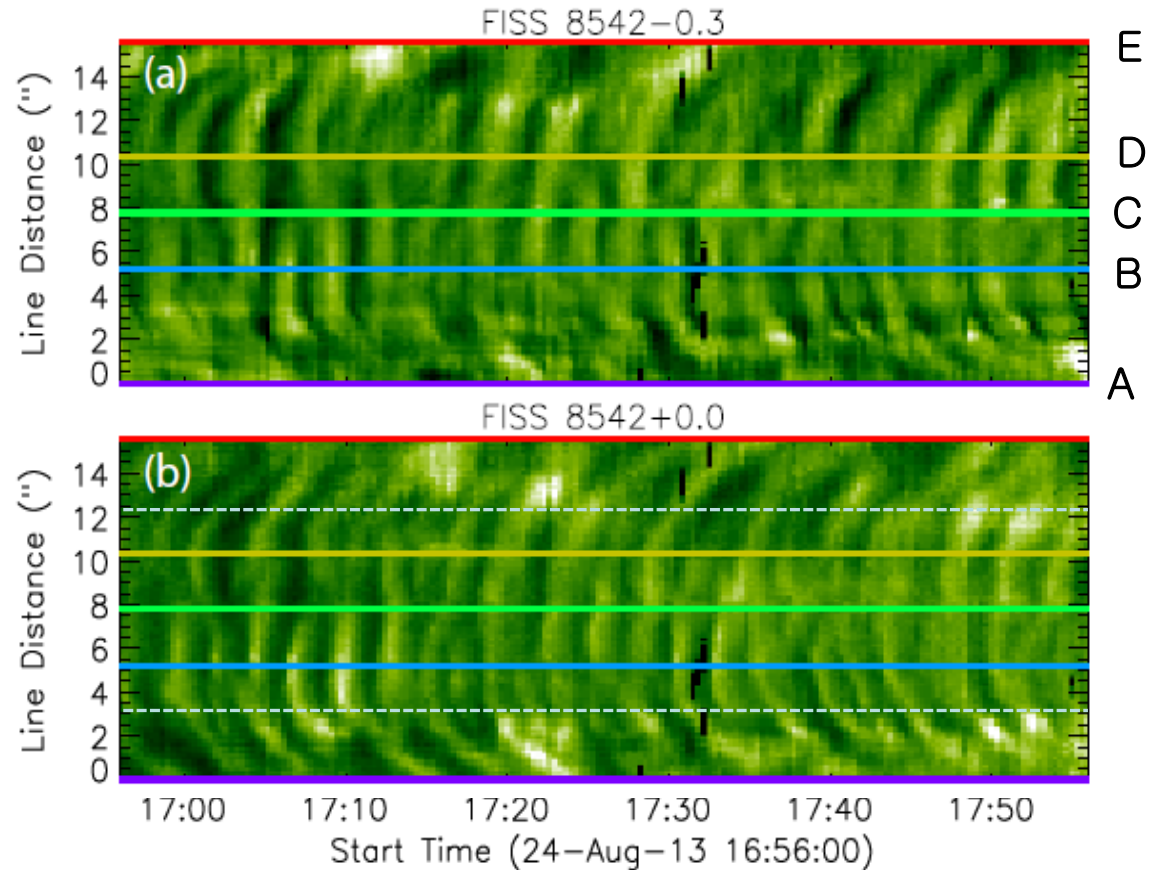
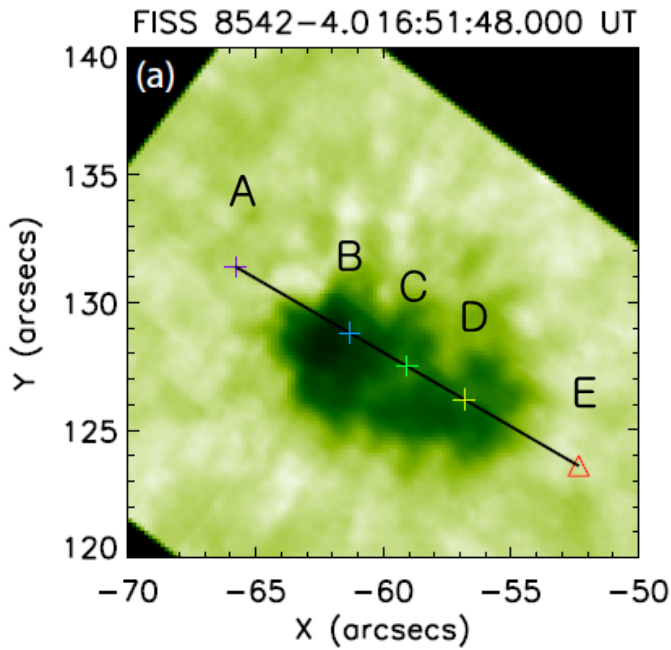
Ha Line center



Ha Line wing

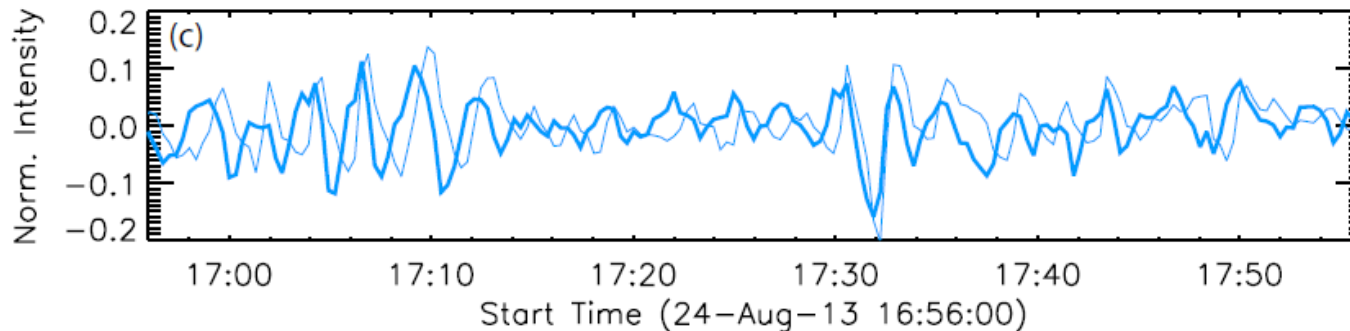


Wave source and propagation in CaII



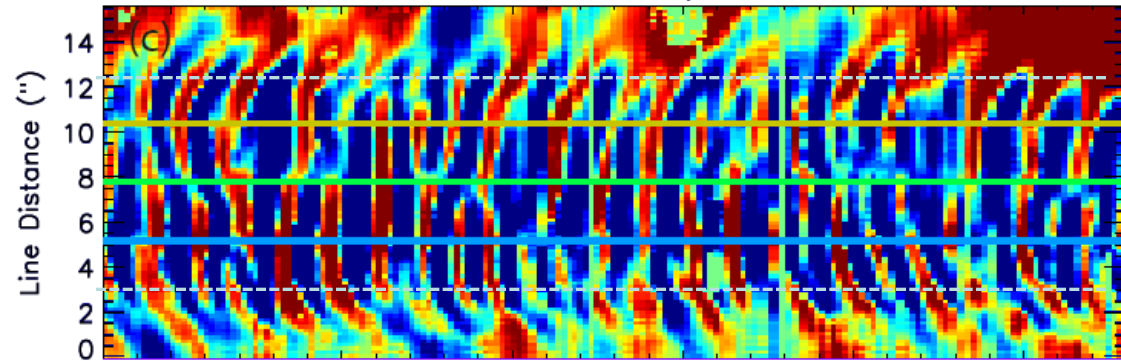
Thick line
: -0.3\AA

Thin line
: -0.0\AA

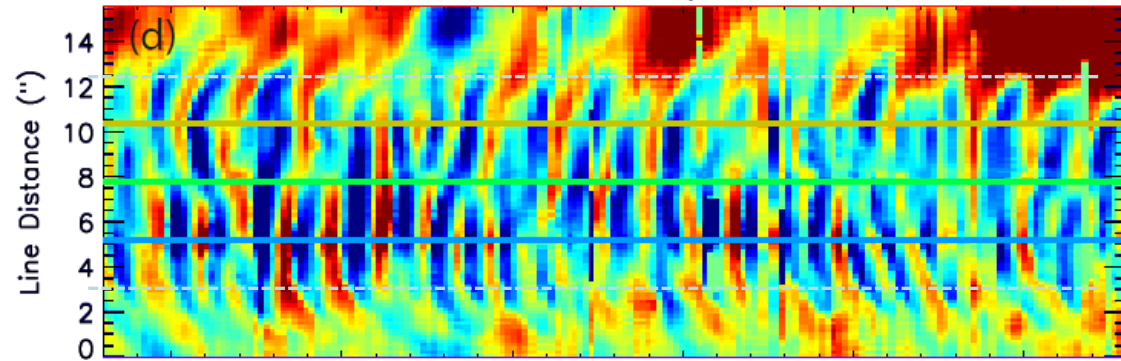


Wave source and propagation in H α

FISS 6562.8 DopLev0

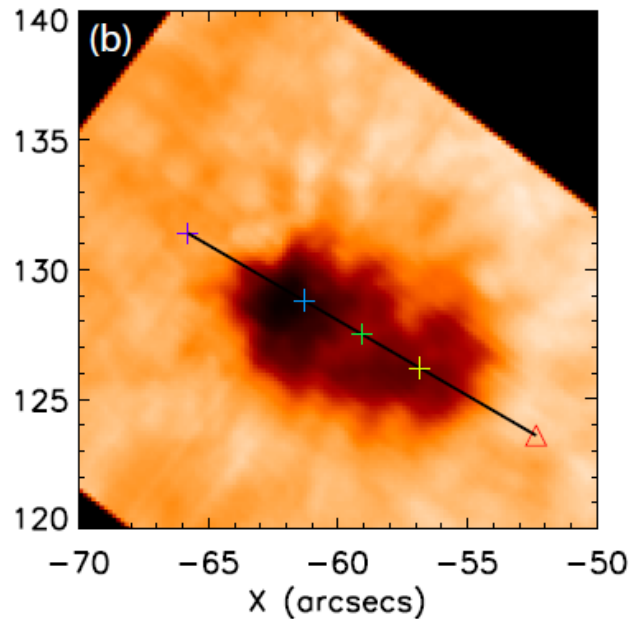


FISS 6562.8 DopLev1

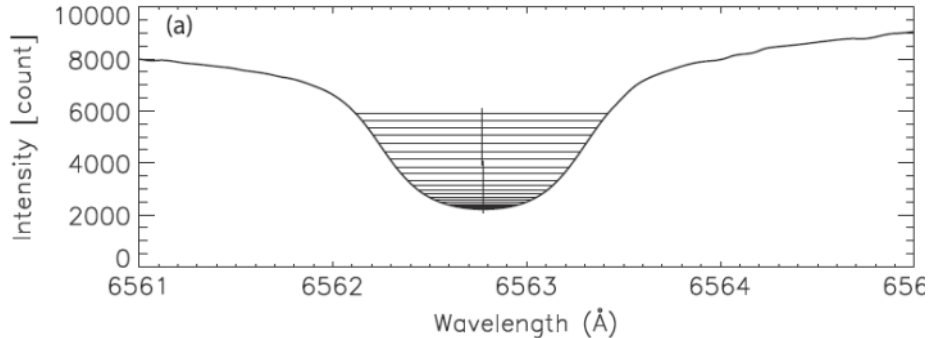


Start Time (24-Aug-13 16:56:00)

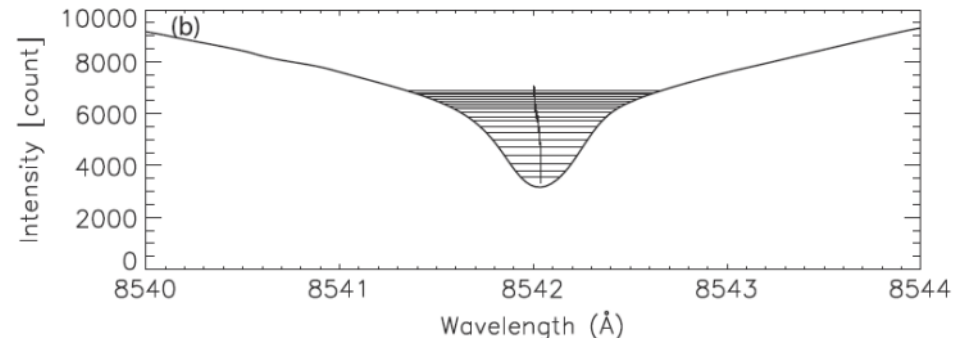
FISS 6562.8-4.0 16:51:48.000 UT



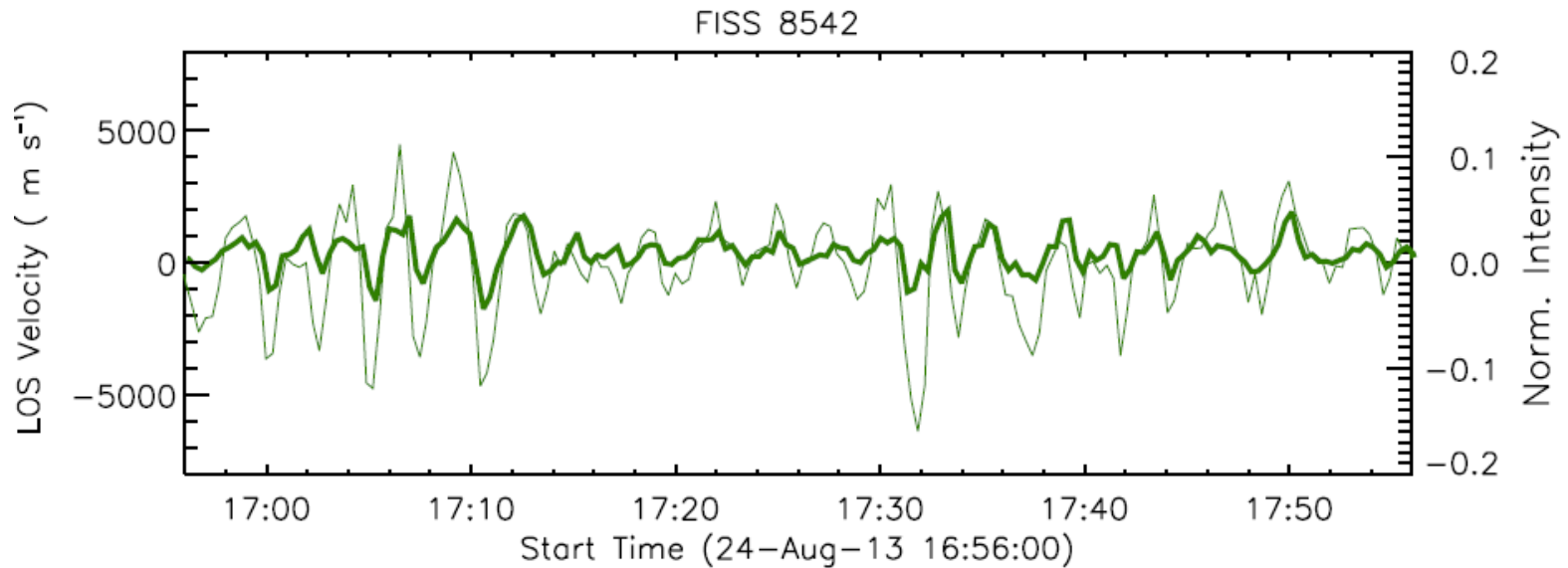
H α



Ca II

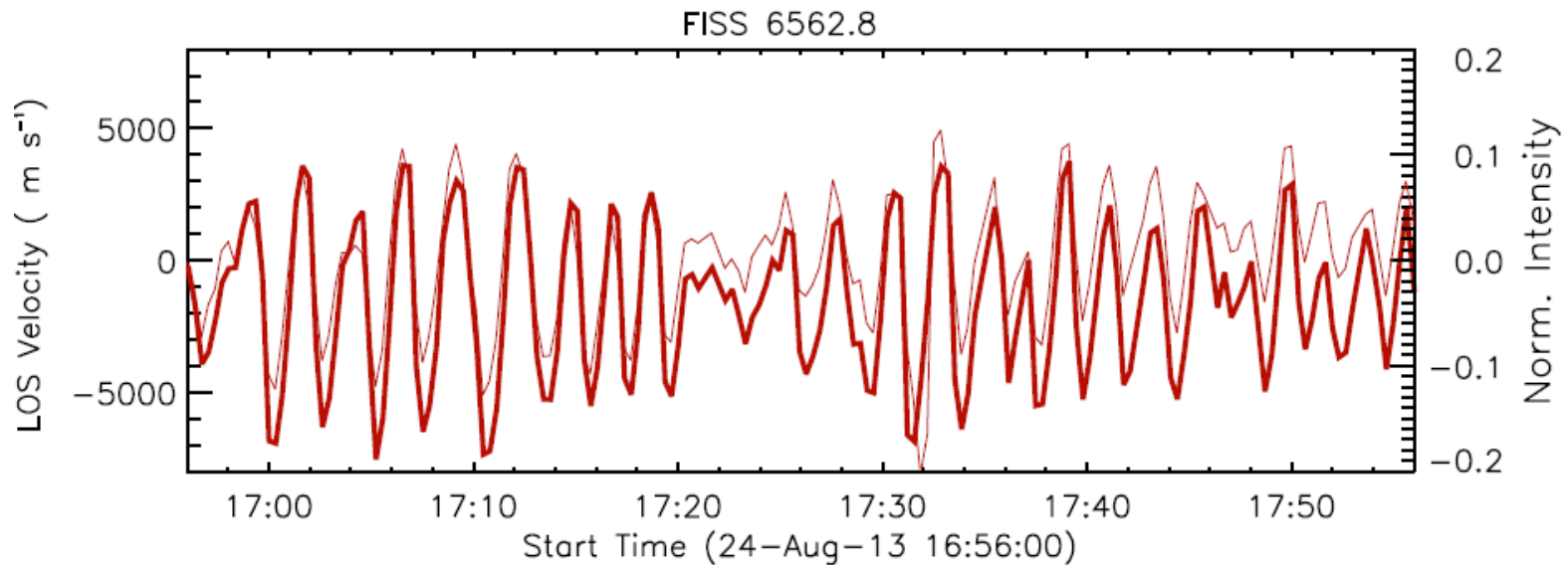


LOS speed and Intensity comparison at Ha (-0.3Å) and CaII (-0.3Å)

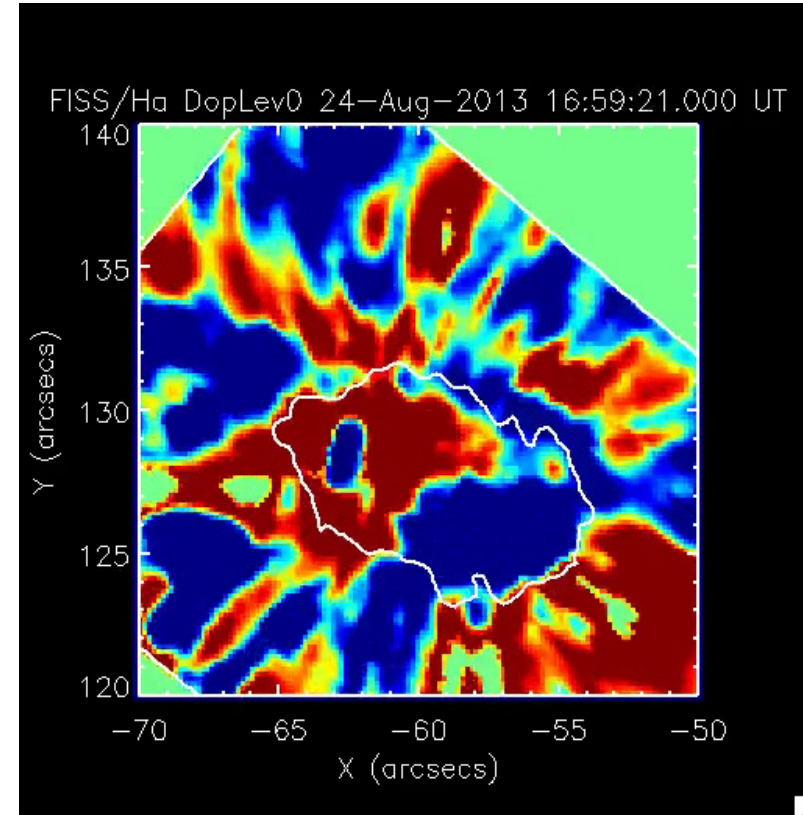
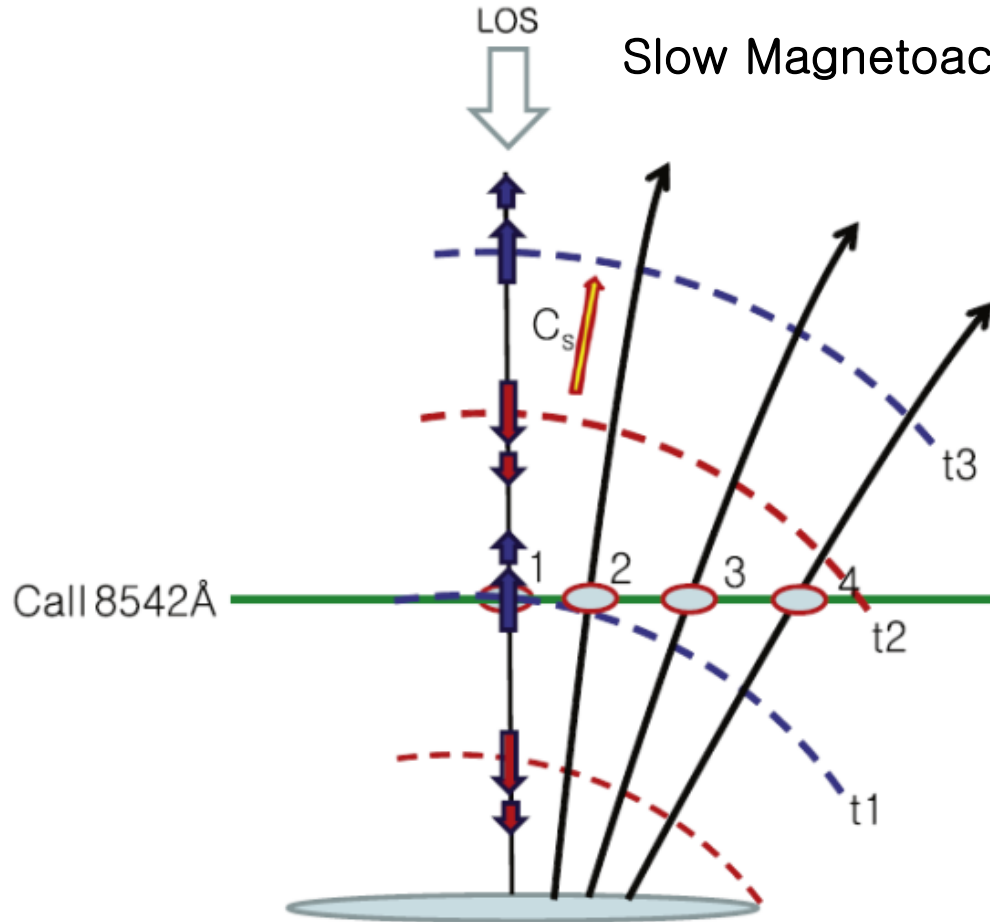


Thick line
: Doppler speed

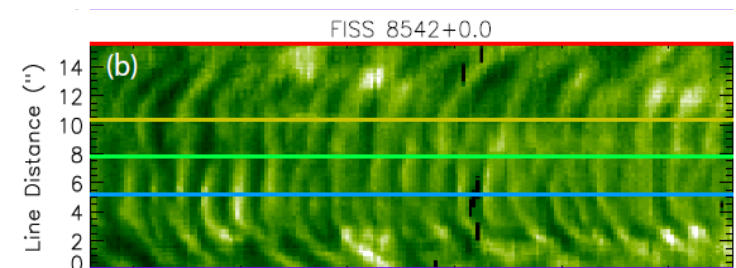
Thin line
: Intensity



Conclusion (Cho et al., 2015)

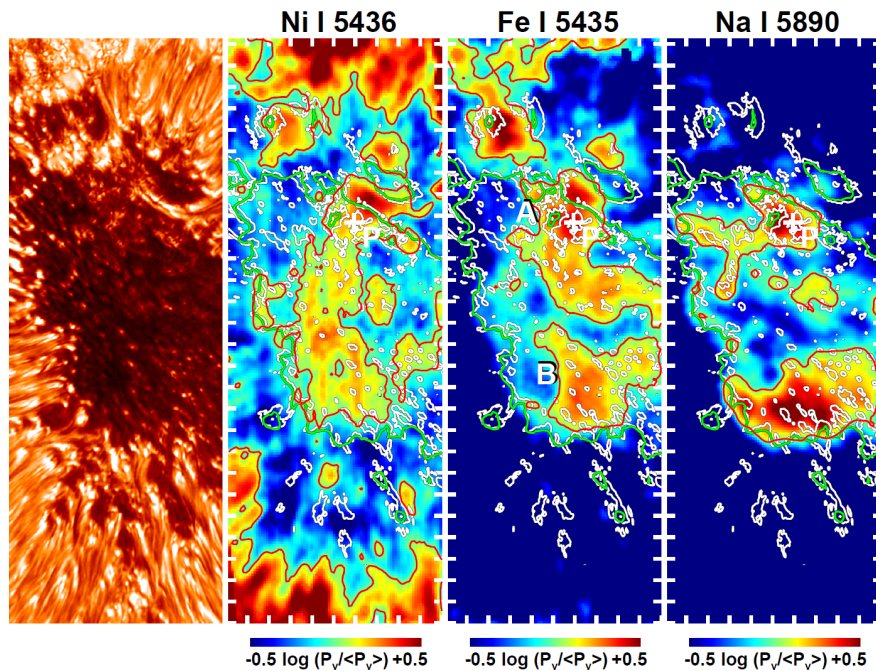


Sudden decrease of its speed beyond the pores can be explained by the **projection effect caused by inclination of the magnetic field** with a canopy structure.

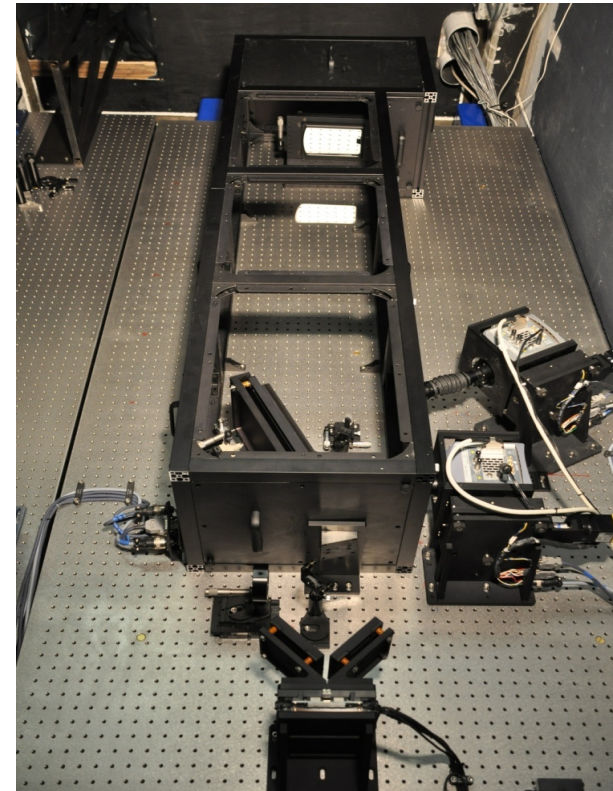


Origin of 3-min UW (Chae et al., 2017)

The local enhancement of the 3-minute oscillation power in the vicinities of a light bridge and numerous umbra dots in the photosphere

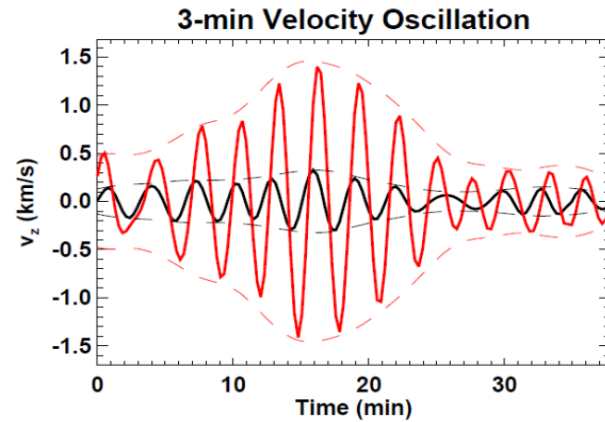
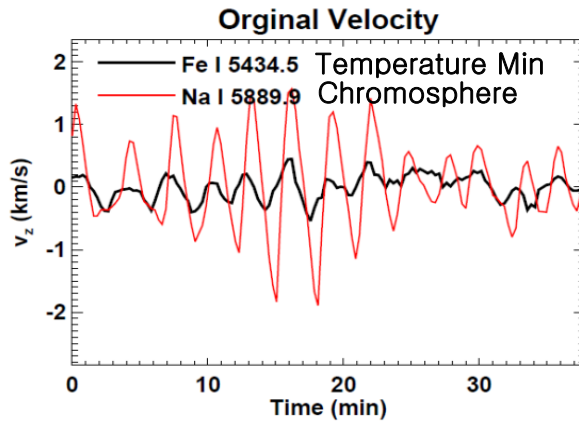


Fast Imaging Solar Spectrograph (FISS)

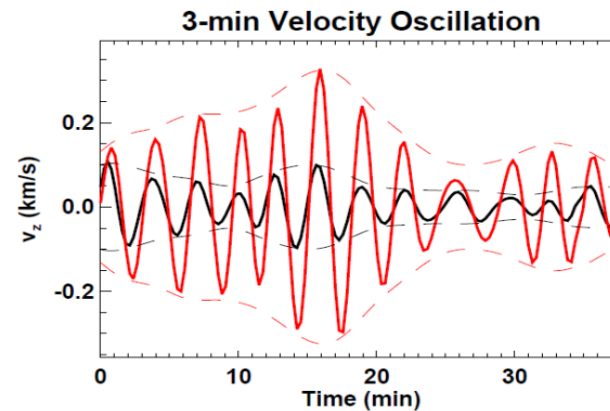
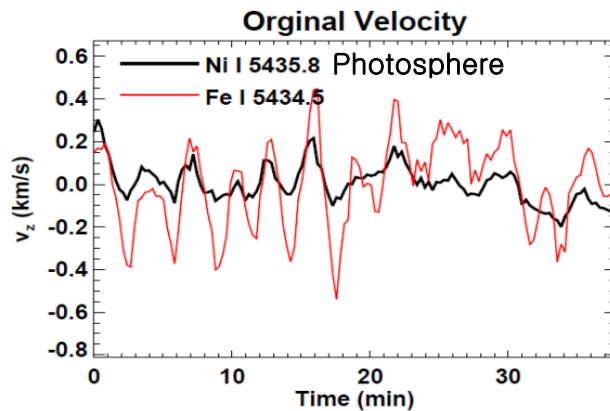


FISS recorded the Na I line on camera A and the Fe I line and Ni I line on camera B simultaneously, which is quite suitable for studying of wave propagation in chromosphere (Na I line), around the temperature minimum (Fe I line), and the photosphere (Ni I line)

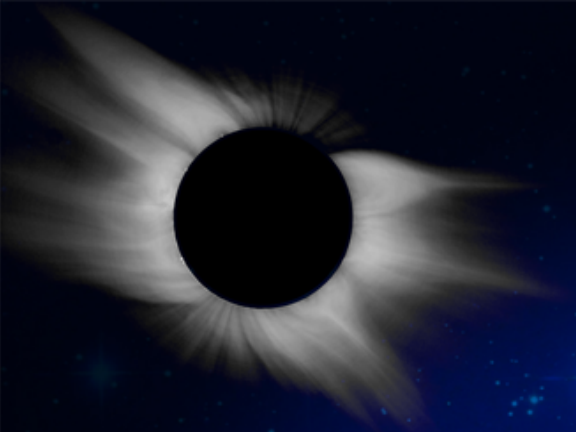
Origin of 3-min UW (Chae et al., 2017)



3-min band
filtered velocity



- (1) 3-min oscillation in the sunspot umbra are persistent in the low atmosphere, even down to the photosphere
- (2) There exist systematic phase differences between different lines that are compatible with the upward propagation of the waves



(2) Photosphere Observation using SDO/HMI



KASI SDO Website (<http://sdo.kasi.re.kr>)

Home Introduction Data Gallery hit counts: 70997

KDC for SDO

Easy Access to SDO Data

KDC for SDO provides a user-friendly web-based service to browse and download the complete set of SDO/AIA and HMI data. It is easy, quick, and convenient!

KDC for SDO

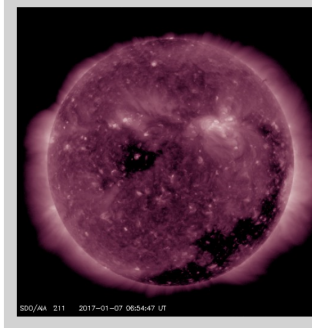
KASI construct a data center for HMI and AIA data. We have compressed Rice FITS data and JPEG2000 data fully. The goal of Korean Data Center for SDO provide easy and fast data access service for researchers in Asia.

Data

- AIA 93, 131, 171, 193, 211, 304, 336, 1600, 1700, 4500
- HMI Magnetogram, Colorized Magnetogram, Intensitygram, Dopplergram
- 4096px, 2048px, 1024px, 512px, 48 hr MPEG
- FITS only available at archive service

[Browse Data](#)

The Sun Now



Courtesy of NASA/SDO and the AIA, EVE, and HMI science teamstt.
Korean Data Center for SDO, Korea astronomy & space science institute.
776 Deadeokdae-ro, Yuseong-gu, Deajeon, 305-348, Rep. of Korea



Data and Process

Korean Data Center for SDO

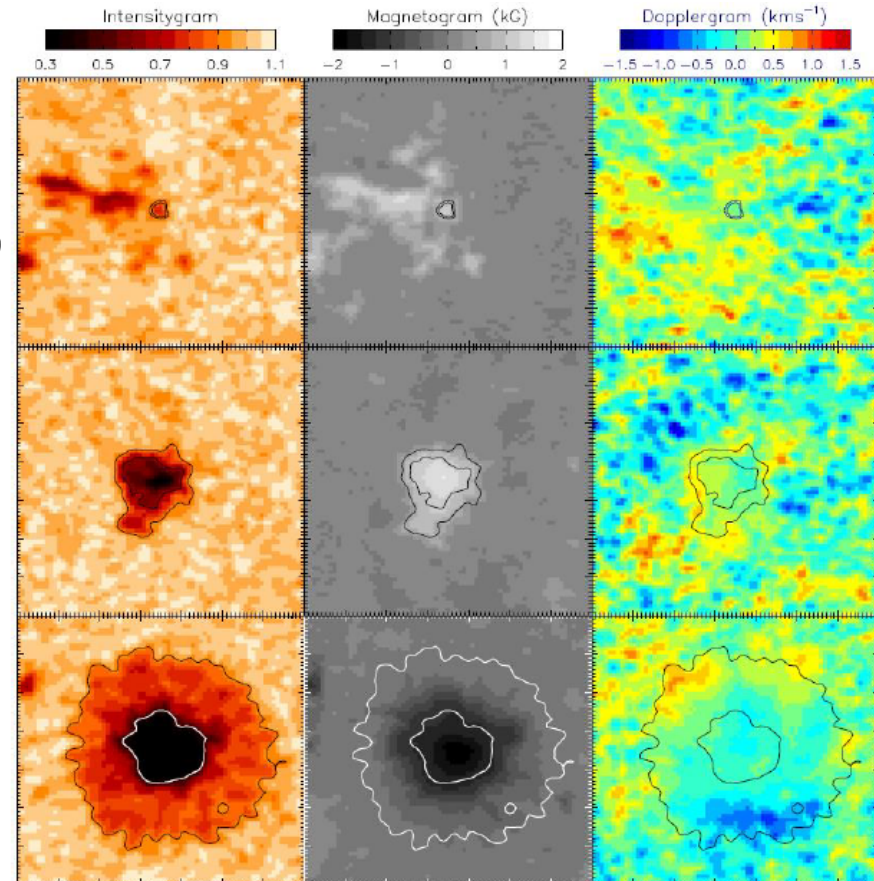
KASI and NASA signed LOA (a letter of agreement) in order to cooperate space science research.

- Daily (00 UT) *SDO*/HMI data
(May 2010 – Feb 2015, 1663 images)

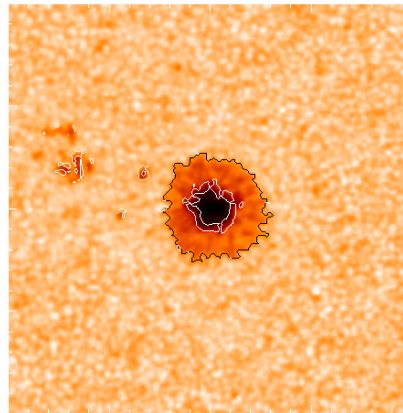
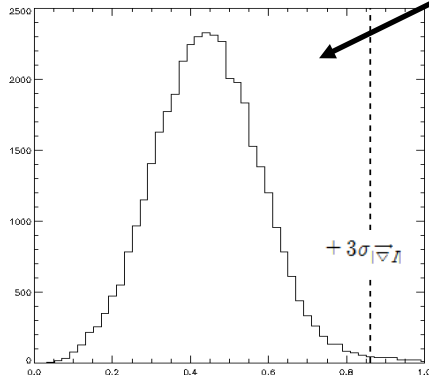
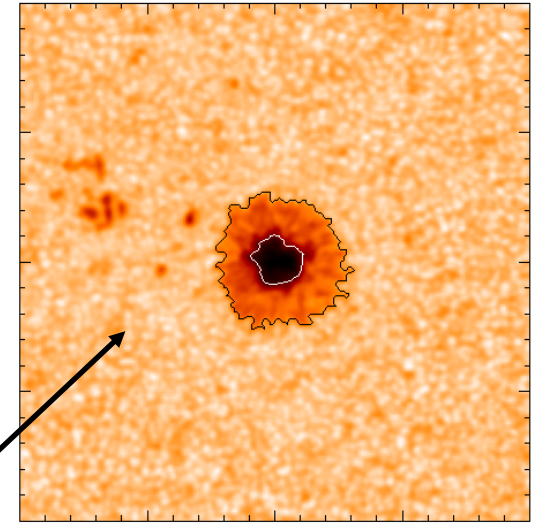
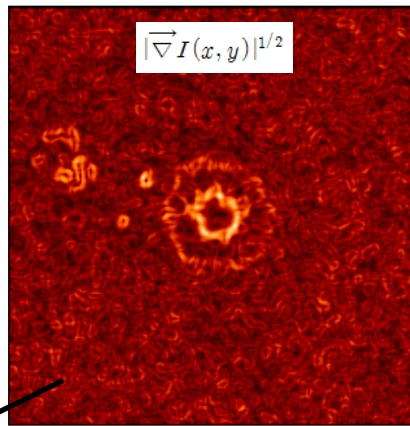
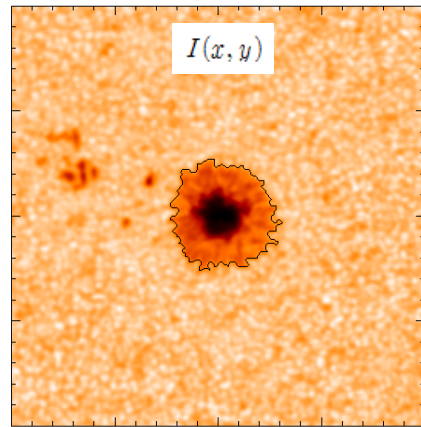
- Radial component

- (1) Remove proper motion of the SDO satellite
- (2) Use $\cos \mu > 0.87$
- (3) Remove solar differential rotation
- (4) de-projection
- (5) remove supergranular vertical motion

- Sunspot boundaries



Sunspot boundaries



A_{Outer}	I_{Outer}	B_{Outer}	V_{Outer}
A_{Inner}	I_{Inner}	B_{Inner}	V_{Inner}

Result: Magnetic flux vs. Area

265,542 Dark holes

A_{Outer} I_{Outer} B_{Outer} V_{Outer}
 A_{Inner} I_{Inner} B_{Inner} V_{Inner}

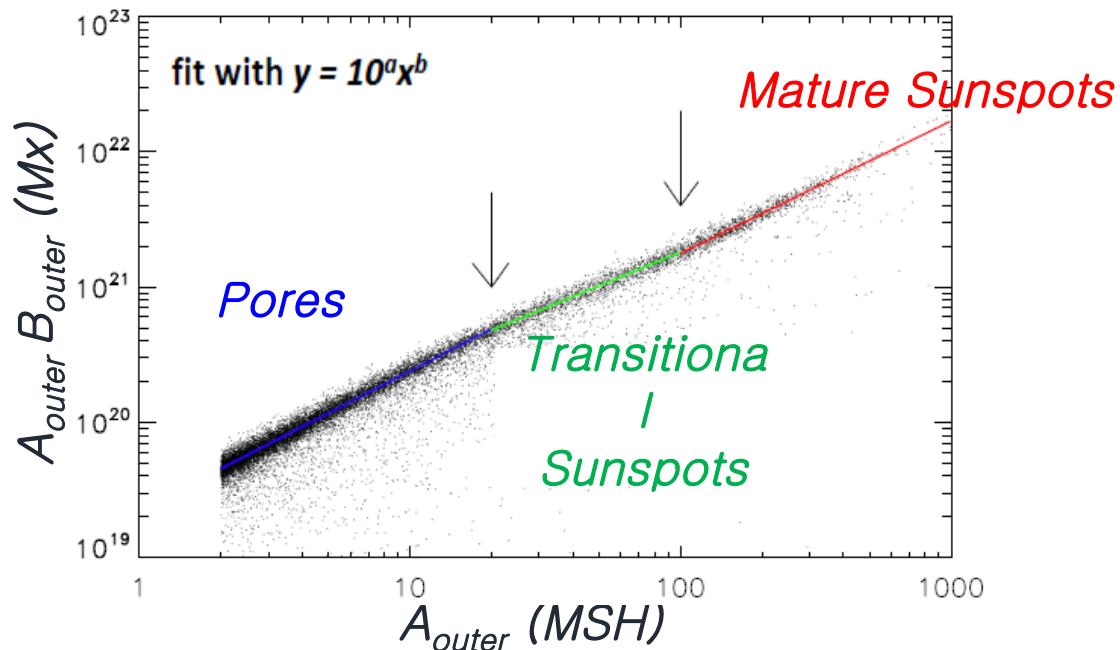


9881 Sunspots

($A_{outer} > 2$ MSH, $B > 500$ G)

$$1 \text{ SH} = 2\pi R_{\text{Sun}}^2$$

($\sim 3 \text{ Mm}^2 \sim 1.7 \times 1.7 \text{ km}$)



$$1.0232 \pm 0.0056$$

$$b = 0.8089 \pm 0.0165$$

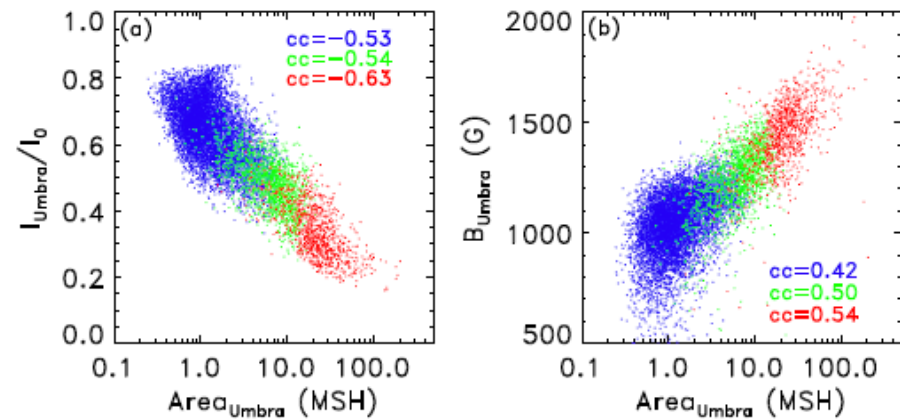
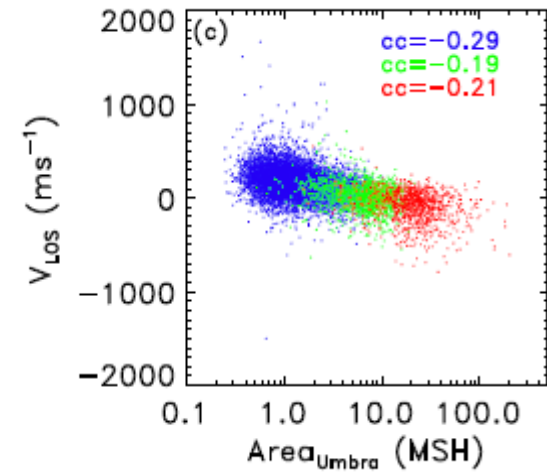
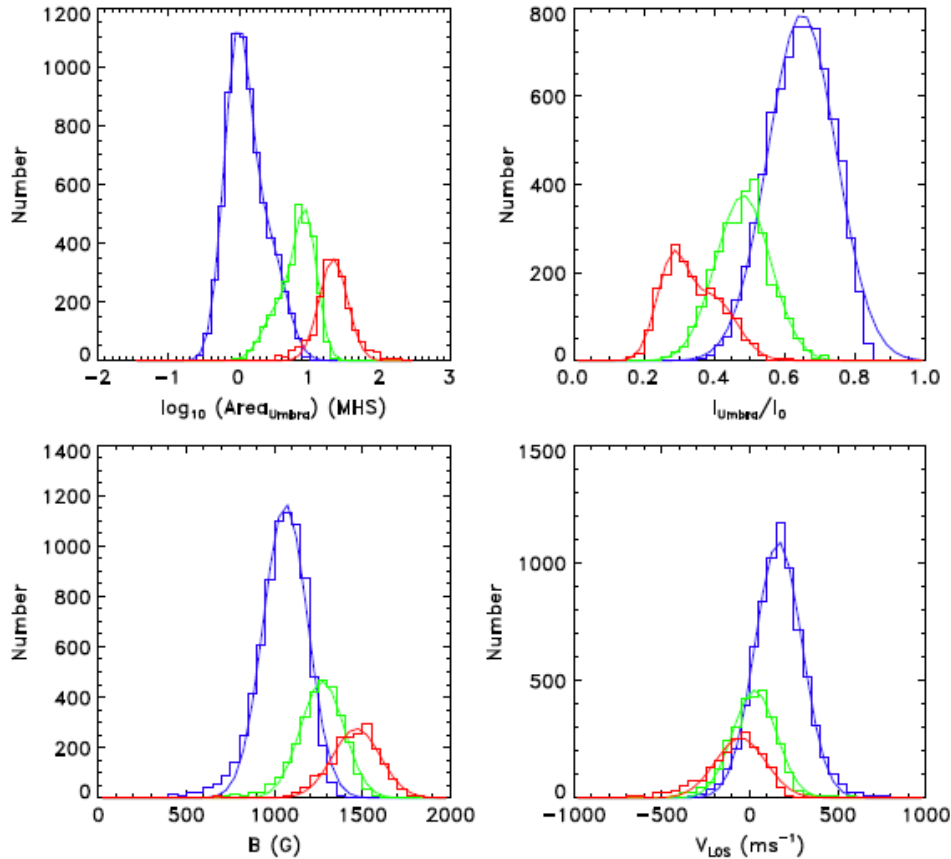
$$0.9989 \pm 0.0219$$

Classification: 20 – 100
MSH
Tlatov & Pevstov (2014)



MSH: Millionth of the Solar Hemisphere

Results (Cho et al., 2016)



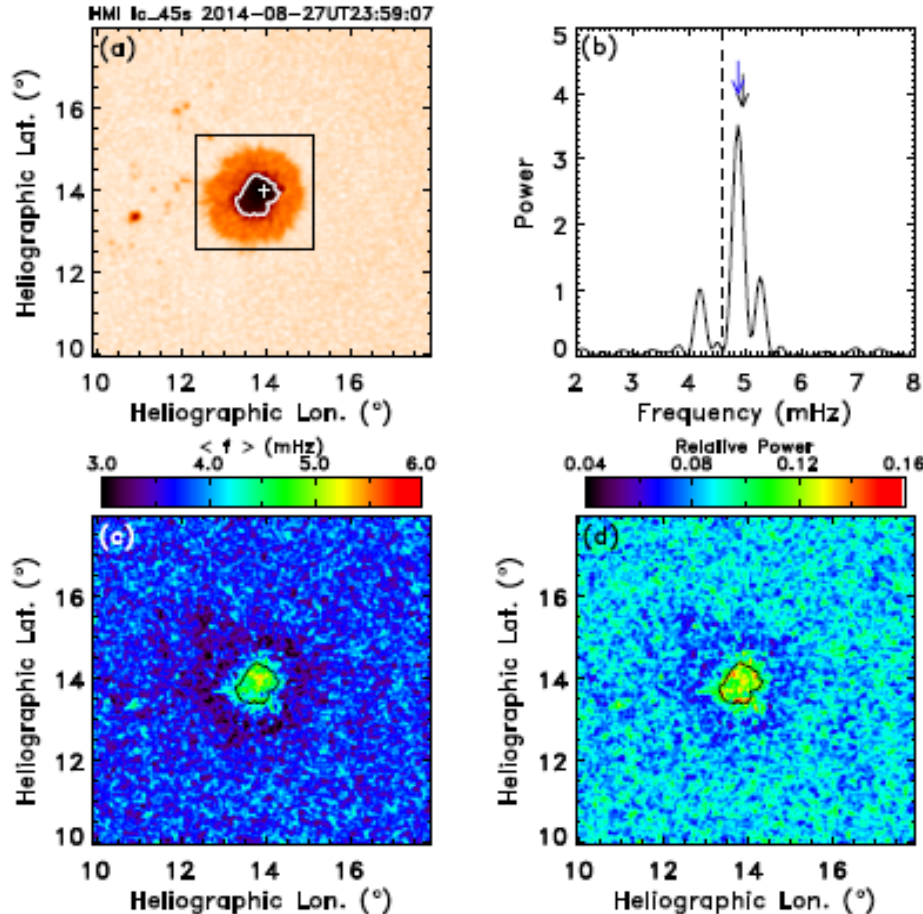
**Bimodal distributions of
I, B, Vlos**

**Pores: redshifted
Sunspots: blueshifted**

Determination of V_A and plasma- β

- Applying seismology based on the theory of slow magnetoacoustic waves in the non-isothermal stratosphere with a uniform vertical magnetic field, we estimated the Alfvén speed, plasma beta, and mass density within umbra.
- Select 478 central ($\cos \mu > 0.954$) sunspot cubes (1-hour) with Area > 5 MSH
- $I = I_{obs} / I_{quiet}$ with even spacing by using the bilinear interpolation
($I_{xy} = I_{00} (1-x)(1-y) + I_{10} x(1-y) + I_{01} (1-x)y + I_{11} xy$)

Weighted Mean Frequency



$$\langle f \rangle = \frac{\sum P(f) f}{\sum P(f)}$$

Using $\langle f \rangle$ rather than f_{Peak}

- Multiple peaks
- Spatial dependency of dominant frequency (Reznikov et al. 2012, Kobanov et al. 2011)

Method: Seismology

-Non-isothermal, stratified atmosphere with a uniform vertical magnetic field

(Roberts 2006)

$$\Omega^2 = (2\pi f_{cutoff})^2 = c_T^2 \left\{ \frac{1}{4\Lambda_p^2} \left(\frac{c_T}{c_S} \right)^4 - \frac{1}{2} \gamma g \left(\frac{c_T}{c_S} \right)' + \frac{1}{c_A^2} \left(\omega_g^2 + \frac{g}{\Lambda_p} \frac{c_T^2}{c_S^2} \right) \right\} \quad \omega_g^2 = g/\Lambda_p - g^2/c_S^2, \quad \Lambda_p = c_S^2/(\gamma g)$$

Reformulating above equation with respect to X

$$\Omega^2 = (2\pi f_{cutoff})^2 = \frac{3\gamma g}{4\Lambda_p} X^3 + \left(\frac{\gamma g}{2\Lambda_p} - \frac{\gamma g}{\Lambda_p} - \frac{g}{\Lambda_p} \right) X^2 + \left(\frac{g}{\Lambda_p} - \frac{g}{\Lambda_p} + \frac{g}{\gamma\Lambda_p} \right) X + \frac{g}{\Lambda_p} - \frac{g}{\gamma\Lambda_p} \quad X \equiv c_T^2/c_S^2$$

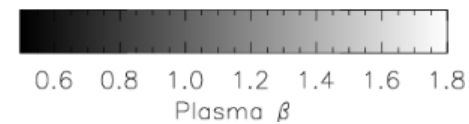
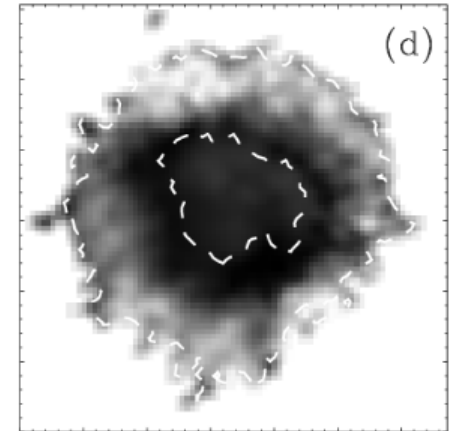
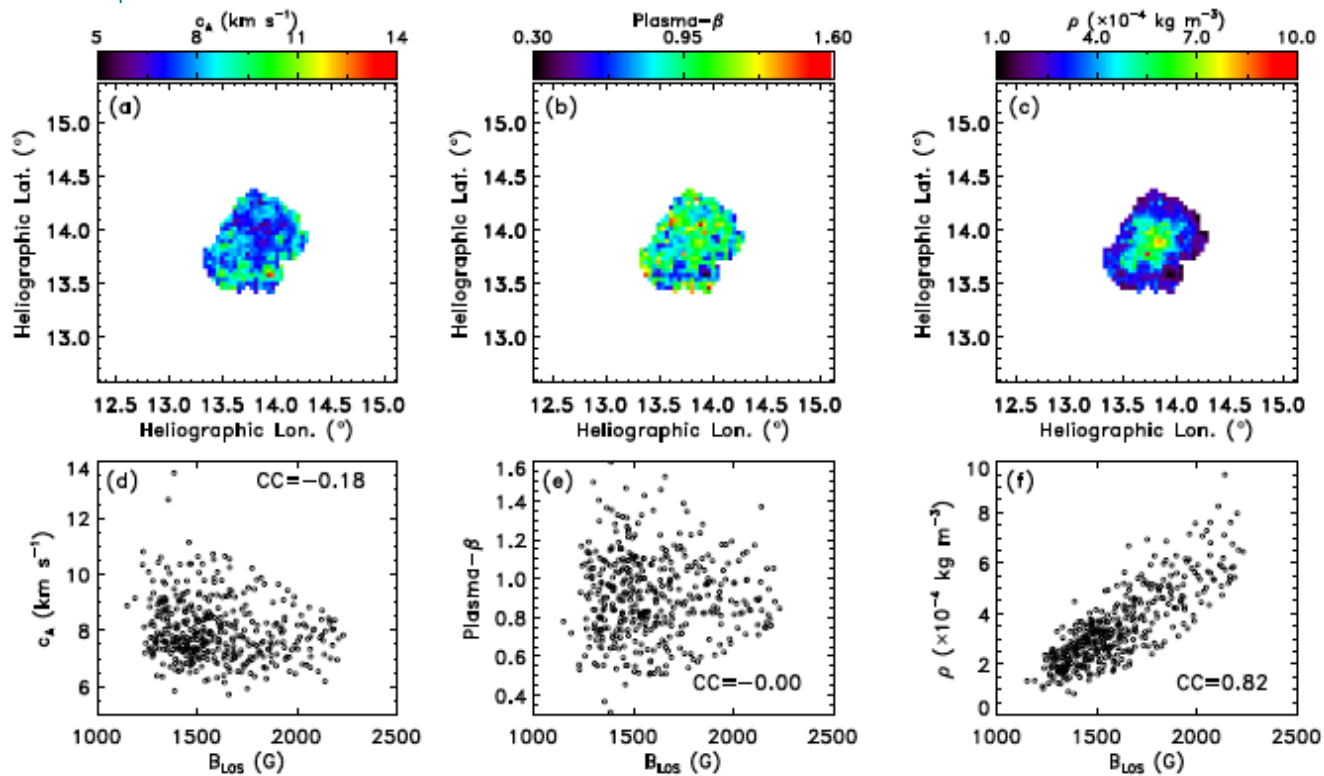
$I/I_0 \rightarrow T$ (Plank's law)

$$\rightarrow c_S = [\gamma k_B T / (\mu m_H)]^{1/2} = 103.26 [T]^{1/2}, \quad \Lambda_p = c_S^2 / (\gamma g), \\ \gamma = 5/3, \quad \mu = 1.3, \quad \Lambda_p = \gamma \Lambda_p$$

$$\rightarrow \Omega = \Omega(c_S, c_T) = \Omega_{obs}, \quad f_{cutoff} = 0.55 \langle f \rangle$$

We found that positive solutions for all pixels inside the umbra exist when the scaling is in 0.5–0.55. Thus we take 0.55 as the upper limit of the scaling.

Result: Map of plasma- β

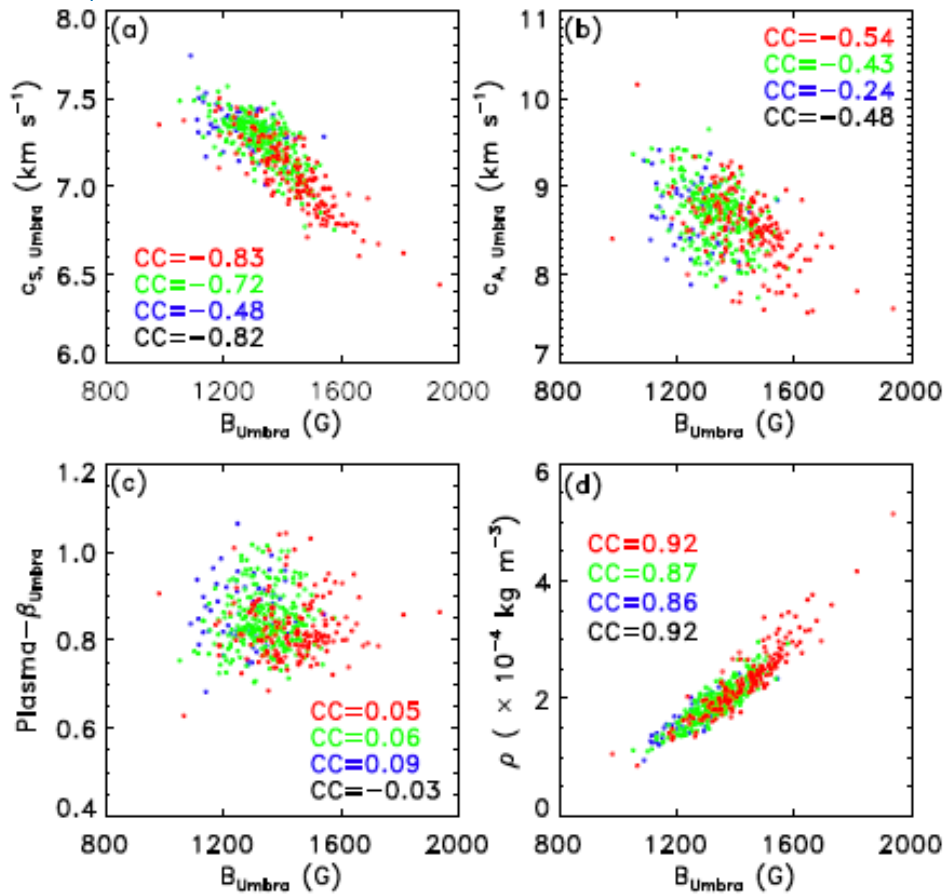


c.f., Mathew & Solanki (2004)

$$X \equiv c_T^2 / c_S^2 \Rightarrow c_A = c_S c_T / [c_S - c_T]^{1/2}, \beta = 2 c_S^2 / (\gamma c_A^2), \rho_o = B_o^2 / [\mu c_A^2]^{1/2}$$

Result: plasma β and C_A vs. B

Result – Average Plasma- β and c_A vs. B for 478 umbrae



- Pores (< 20 MSH)
- Transitional sunspots ($20 - 100$ MSH)
- Mature sunspots (> 100 MSH)

→ c_A are negatively correlated with B , which might be due to significant increase of density

→ Plasma- β in umbra seems to be independent of B

→ Density inside the umbra is highly dependent on the field strength.

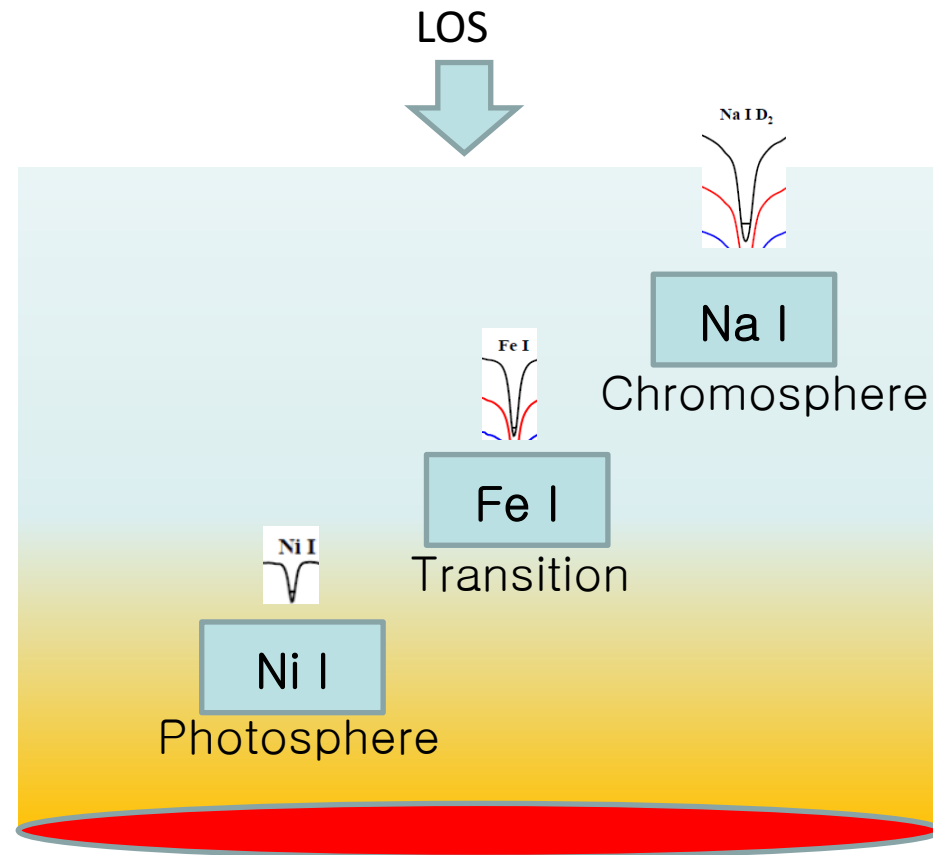
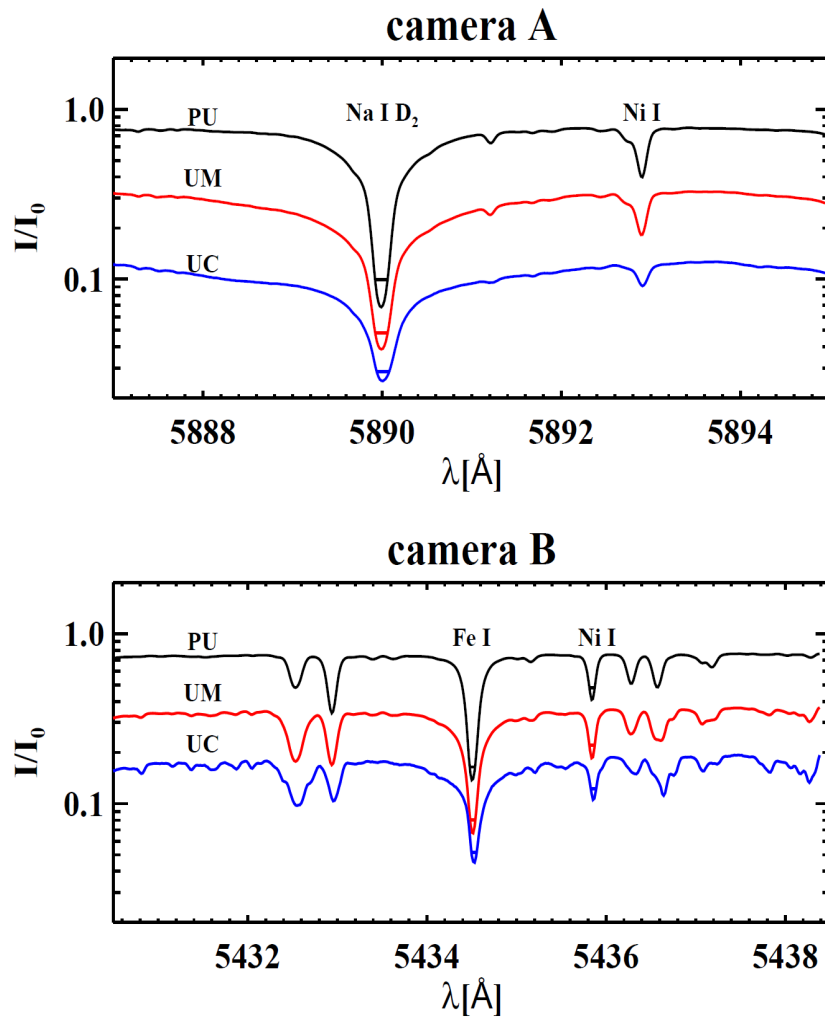
Conclusion

- (1) High resolution imaging spectrograph observations using NST/FISS shows that the observed wave inside umbra is a **slow magnetoacoustic wave propagating along the magnetic field lines** in the pores.
- (2) Three groups of pores, transition sunspots, and mature sunspots have **different characteristics in their area, intensity, magnetic field, and LOS velocity as well in their relationships.**
- (3) **Deduced Alfvén speed** and sound speed inside sunspot umbra is **negatively correlated with average magnetic field strength**, which might reflect **a depression of the continuum forming height.**



Thank you
for your attention

Line formation height



Usually the lower the core intensity of an absorption line is, the higher the line formation region is.